JPET Fast Forward. Published on June 26, 2018 as DOI: 10.1124/jpet.118.248369
This article has not been copyedited and formatted. The final version may differ from this version.

Title Page

Contributions of Nrf2 to puerarin prevent cardiac hypertrophy and its metabolic enzymes expression in rats

Gan-Jian Zhao[1], Ning Hou[1], Shao-Ai Cai[1], Xia-Wen Liu[1], Ai-Qun Li, Chuan-Fang Cheng, Yin Huang, Li-Rong Li, Yun-Pei Mai, Shi-Ming Liu, Cai-Wen Ou, Zhen-Yu Xiong, Xiao-Hui Chen, Min-Sheng Chen, Cheng-Feng Luo

The Second Affiliated Hospital of Guangzhou Medical University, Guangzhou Institute of Cardiovascular Disease, Guangzhou, China.(GJZ, AQL,CFC, YH, LRL, SML, CFL)

School of Pharmaceutical Sciences and the Fifth Affiliated Hospital, Guangzhou Medical University, Guangzhou, China. (NH, XWL, YPM)

The Second Affiliated Hospital of Guangzhou Medical University, Guangzhou, China. (SAC, XHC)

Zhujiang Hospital, Southern Medical University, Guangdong provincial Center of Biomedical Engineering for Cardiovascular Disease, Guangzhou, China.(CWO, MSC)

Guangdong Second Provincial General Hospital, Guangzhou, China. (ZYX)

JPET Fast Forward. Published on June 26, 2018 as DOI: 10.1124/jpet.118.248369
This article has not been copyedited and formatted. The final version may differ from this version.

Running title page

Runing title: Contributions of Nrf2 to puerarin prevent cardiac hypertrophy

Corresponding authors:

Cheng-Feng Luo, Department of Cardiology, The Second Affiliated Hospital of Guangzhou Medical University, Guangzhou Institute of Cardiovascular Disease, 250 Changgangdong Road, Guangzhou 510260, China. E-mail address: rocenphone@gzhmu.edu.cn.

Min-Sheng Chen, Department of Cardiology, Zhujiang Hospital, Southern Medical University, Guangdong provincial Center of Biomedical Engineering for Cardiovascular Disease, No. 1023, Shatai Nan Road, Guangzhou 510280, China. E-mail address: gzminsheng@vip.163.com.

Contents:

Text page count: 46

Table count: 1

Figure count: 8

Reference count: 39

Word Count: Abstract: 253

Introduction: 591

Discussion: 1071

Abbreviations:

AAC, abdominal aortic constriction; AhR, aryl hydrocarbon receptor; AngII: angiotensin Ⅱ; ANP, atrial natriuretic peptide; ARE, antioxidant/electrophile-response

JPET Fast Forward. Published on June 26, 2018 as DOI: 10.1124/jpet.118.248369
This article has not been copyedited and formatted. The final version may differ from this version.

element; CAR, constitutive androstane receptor; cDNA, Complementary DNA; ChIP, Chromatin immunoprecipitation; GSTP1, glutathione transferase p 1; HO1, heme oxygenase-1; H&E, hematoxylin and eosin; IVSd, interventricular septum; LVEDP: left ventricular end-diastolic pressure; LVEF, left ventricular ejection fraction; LVESP, left ventricular end-systolic pressure; LVFS, left ventricular fractional shortening; LVId, left ventricular interior diameter; LVPWd, Left ventricular posterior wall diameter; Nrf2, nuclear factor erythroid 2-related factor 2; NRCMs, neonatal rat cardiomyocytes; NQO1, NAD(P)H:quinone oxidoreductase 1; PSR, picrosirius red staining; PXR, pregnane X receptor; UGTs, UDP-glucuronosyltransferases.

JPET Fast Forward. Published on June 26, 2018 as DOI: 10.1124/jpet.118.248369
This article has not been copyedited and formatted. The final version may differ from this version.

Abstract

Previous evidence suggested that puerarin may attenuate cardiac hypertrophy; however, the potential mechanisms were undetermined. Moreover, the use of puerarin is limited by severe adverse events, including intravascular hemolysis. This study used a rat model of abdominal aortic constriction (AAC)-induced cardiac hypertrophy to evaluate the potential mechanisms underlying the attenuating efficacy of puerarin on cardiac hypertrophy as well as the metabolic mechanisms of puerarin involved. We confirmed that puerarin (50 mg/kg/d) significantly attenuated cardiac hypertrophy, upregulated Nrf2 and decreased Keap1 in the myocardium. Moreover, puerarin significantly promoted Nrf2 nuclear accumulation in parallel with the upregulated downstream proteins including heme oxygenase 1, glutathione transferase P1 and NAD(P)H: quinone oxidoreductase 1. Similar results were obtained in neonatal rat cardiomyocytes (NRCMs) treated with angiotensin II (1 μM) and puerarin (100 μM), while the silencing of Nrf2 abolished the antihypertrophic effects of puerarin. The mRNA and protein levels of UGT1A1 and UGT1A9, enzymes for puerarin metabolism, were significantly increased in the liver and heart tissues of AAC rats and angiotensin II-treated NRCMs. Interestingly, the silencing of Nrf2 attenuated the puerarin-induced upregulation of UGT1A1 and UGT1A9. The results of chromatin immunoprecipitation–qPCR indicated that the binding of Nrf2 to the promoter region of *Ugt1a1 or Ugt1a9* was significantly enhanced in puerarin-treated cardiomyocytes. These results suggest that Nrf2 is the key regulator of antihypertrophic effects and the

JPET Fast Forward. Published on June 26, 2018 as DOI: 10.1124/jpet.118.248369
This article has not been copyedited and formatted. The final version may differ from this version.

upregulation of the metabolic enzymes UGT1A1 and UGT1A9 of puerarin. This autoregulatory circuits between puerarin and Nrf2-induced UGT1A1/1A9 are beneficial to attenuate adverse effects and maintain the pharmacological effects of puerarin.

Keywords: puerarin; cardiac hypertrophy; Nrf2; UGT1A1/1A9; metabolic feedback loop

JPET Fast Forward. Published on June 26, 2018 as DOI: 10.1124/jpet.118.248369
This article has not been copyedited and formatted. The final version may differ from this version.

1. Introduction

Puerarin (7,4′-dihydroxyisoflavone-8β-glucopyranoside) is a major active ingredient in Chinese medicine Pueraria radix, which is extracted from the kudzu root (Pueraria lobota (Wild) Howe). The pharmacological benefits of puerarin include improvement of microcirculation, scavenging of oxygen free radicals, and amelioration of insulin resistance (Zhou et al., 2014b), which make it a potential treatment for patients with hypertension (Song et al., 1988), cerebral ischemia (Gao et al., 2009), myocardial ischemia (Zhang et al., 2006), diabetes mellitus (Hsu et al., 2003), and arteriosclerosis (Yan et al., 2006).

Physiologically, cardiac tissue exhibits plasticity that enables the heart to respond to various physiological or pathological stresses. Under the continuous stress induced by pathological conditions including hypertension and aortic stenosis, pathological hypertrophy is characterized by ventricular remodeling, with the impairment of cardiac systolic and diastolic function, which eventually lead to deleterious outcomes, such as heart failure, arrhythmia, and sudden cardiac death (Oka et al., 2014; Kamo et al., 2015). Therefore, preventative strategies against the incidence of pathological cardiac hypertrophy may be important to improve the outcome in patients at risk of developing heart failure. Puerarin has been suggested to confer antihypertrophic efficacy in the heart (Yuan et al., 2014; Liu et al., 2015). Results of our previous

studies showed that puerarin may prevent cardiac hypertrophy via the restoration of the AMPK/mTOR-mediated autophagy pathway (Liu et al., 2015). Moreover, other studies showed that puerarin may exert antihypertrophic efficacy via other mechanisms, such as the blockade of hypertrophy-related signaling pathways (Chen et al., 2014; Yuan et al., 2014), the inhibition of oxidative stress (Chen et al., 2015; Hou et al., 2017), and the enhancement of miR-15b and miR-195 expression (Zhang et al., 2016). However, the key regulator that is involved in the potential antihypertrophic efficacy of puerarin remains to be determined.

Understanding the metabolic pathways of puerarin is important to optimize its pharmacological efficacy and to limit its potential adverse effects. Puerarin has a very low water solubility with a limited absolute bioavailability of 1.8% after oral administration (Luo et al., 2011a; Luo et al., 2011b; Li et al., 2014). Generally, xenobiotics experience absorption, metabolism, disposition, and excretion after administration. Puerarin-7-*O*-glucuronide is one of the major metabolites of puerarin in rats (Luo et al., 2012; Luo et al., 2013). Our previous studies confirmed that seven UDP-glucuronosyltransferase (UGT) isoforms (UGT1A1, 1A9, 1A10, 1A3, 1A6, 1A7, and 1A8) can catalyze the formation of its major metabolite, puerarin-7-*O*-glucuronide, and UGT1A1 is the primary enzyme responsible for the metabolism of puerarin (Luo et al., 2012). Moreover, transcription factors such as constitutive androstane receptor (CAR), pregnane X receptor (PXR), and aryl hydrocarbon receptor (AhR), can enhance the transcriptions of UGT isoforms,

including UGT1A1 (Sugatani et al., 2005; Mackenzie et al., 2010). However, recent evidence suggests that the transcription factor nuclear factor erythroid 2-related factor 2 (Nrf2) plays a key role in preserving cardiac function, particularly via the regulation of cardiac hypertrophy, evidenced by the enhanced cardiac hypertrophy and diastolic dysfunction in Nrf2 knockout mice (Erkens et al., 2015). Therefore, we hypothesized that puerarin may prevent cardiac hypertrophy by enhancing the activity of Nrf2. Therefore, the aim of the current study was to investigate whether the potential antihypertrophic efficacy of puerarin is associated with the regulatory effect of Nrf2 in a pressure-overload rat model and angiotensin II-treated neonatal rat cardiomyocytes. Moreover, we aimed to evaluate whether puerarin may also induce UGT1A1 and 1A9 in liver and heart tissue via the regulation of Nrf2. Our results showed that Nrf2 is a common transcription factor in effects of puerarin and that it protects against cardiac hypertrophy and regulates puerarin metabolizing enzymes.

2. Materials and Methods

2.1. Chemicals

Injectable puerarin was purchased from Zhejiang Zhenyuan Pharmaceutical Co., Ltd. (Shaoxing, China). Puerarin and Ang II were purchased from Sigma Chemical (St. Louis, MO, USA). SuperSignal™ West Pico Chemiluminescent Substrate was obtained from Thermo (Rockford, IL, USA). TRIzol® Reagent was purchased from Ambion Inc. (Life Technologies Inc.). A First-Strand cDNA Synthesis Kit was

purchased from Takara. The Coomassie Protein Assay kit was purchased from Bio-Rad Laboratories (Hercules, CA).

2.2. Animal model

Half of the male and female pathogen-free Sprague-Dawley rats (150-180 g) were purchased from Guangdong Medical Laboratory Animal Center (Guangzhou, China). All animal experiments were performed according to the EC Directive 86/609/EEC. The protocol of the animal study was reviewed and approved by the Ethics Committee of Guangzhou Medical University before performance. The rats were housed in an environmentally controlled room (temperature, 25 ± 2 ℃; humidity, 60 ± 5 %; 12/12 h dark/light cycle) with access to regular chow diet *ad libitum* for 1 week prior to the experiments. Cardiac hypertrophy was induced by abdominal aortic constriction (AAC), which was modified based on a previously reported procedure (Reddy et al., 1996; Huang et al., 2015; Ku et al., 2016). In brief, the rats were anesthetized using pentobarbital (45mg/kg, intraperitoneal injection). The abdominal aorta was then exposed above the kidneys and constricted at the suprarenal level by a 7-0 silk suture tied around both the aorta and a blunted 18-gauge needle, which was subsequently removed. A similar procedure without abdominal arterial ligation was performed as a sham surgery. Upon completion of the surgery, the rats were injected with Buprenorphine and placed down on a warming pad until they woke. Baseline echocardiography assessment was performed one week after the surgeries, and the rats were randomly divided into 4 groups. The Sham group included sham rats that

received daily intraperitoneal injection (i.p.) of vehicle, the AAC group included AAC rats with vehicle injection daily, the AAC-Pue group included AAC rats with an injection of puerarin (50 mg/kg body weight) daily, the Sham-Pue group included sham rats with an injection of puerarin (50 mg/kg body weight) daily. Each group contained 4 male and 4 female rats. Echocardiography assessments were performed for the rats in each group every 2 weeks. Following the 6 weeks of puerarin administration, the rats were subjected to catheter-based hemodynamic assessment and were sacrificed after hemodynamic assessment. Their heart and liver tissues were extracted and divided for mRNA, protein, histology and immunofluorescence analysis.

2.3. Echocardiography

Cardiac function was evaluated by transthoracic echocardiography with a 250 MHz ultrasound transducer (Vevo 2100, VisualSonics). The rats were sedated using 2% isoflurane and maintained with 1-1.5% isoflurane. The parasternal short axis view (B-mode, M-mode) was obtained, and measurements of cardiac structure and function were performed. Left ventricular posterior wall diameter (LVPWd), left ventricular interior diameter (LVId), and interventricular septum (IVSd) were measured from the LV M-mode tracing at the mid-papillary muscle level, and parameters of the left ventricular ejection fraction (LVEF) and fractional shortening (LVFS) were calculated.

2.4. Non-invasive measurement of blood pressure and catheter-based analysis of hemodynamic parameters

Rat tails were fixed gently and then subjected to a CODA monitor (Kent Scientific). Non-invasive blood pressure was taken at least 5 times for each animal. The mean systolic pressure and diastolic pressure were recorded. For catheter-based hemodynamic measurements, after the rats were anesthetized with 30% urethane, a catheter transducer was inserted via the right carotid artery into the left ventricle. The parameters left ventricular end-systolic pressure (LVESP), left ventricular end-diastolic pressure (LVEDP), maximal rate of pressure development (Max +dP/dt), and maximal rate of pressure decay (Max -dp/dt) were analyzed using the PowerLab system (ADInstruments, Australia) and recorded.

2.5. Histology and Immunohistochemical staining

The rats were weighed and euthanized using cervical dislocation. The hearts were removed and perfused briefly with 10% KCl to arrest the heart in diastole. The hearts were then fixed with 10% formalin and integrated into paraffin. For histological evaluations with hematoxylin and eosin (H&E), Masson's trichrome, picrosirius red (PSR) staining, tissues from four rats of each group were embedded with paraffin and cut into 4 μm sections as previously described (Yuan et al., 2014). For immunohistochemical staining, antigen retrieval was performed in EDTA buffer (pH: 9.0) by heating to 99 ℃ for 20 minutes. After quenching endogenous peroxidase with 3% H_2O_2, the sections were blocked with 10% non-immune goat serum (Life

Technologies, Grand Island, NY) and then incubated with primary antibodies including NRF2, KEAP1, UGT1A1 or UGT1A9, as shown in Tab. S1 at 4℃ overnight. Signals were amplified with the Histostain-SP Kit (Life Technologies, Grand Island, NY) and detected with DAB substrate (Dako North America, Inc., Carpinteria, CA). Hematoxylin was used as a counterstain. The images were visualized and captured under a microscope (Nikon Eclipse TS 100; Japan).

2.6. Isolation, culture, and treatment of neonatal rat cardiomyocytes

The neonatal rat cardiomyocytes (NRCMs) were isolated from neonatal Sprague Dawley rats (one to two days old) with the assistance of the Neonatal Cardiomyocyte Isolation System purchased from Worthington (Lakewood, NJ, USA) based on the Simpson method (Simpson and Savion, 1982) as previously reported (Hou et al., 2017). The isolated NRCMs were seeded with a density of 5×10^6 cells/ml in DMEM medium containing 10% FBS and 0.1 mM bromodeoxyuridine. The NRCMs were then treated with vehicle alone, Ang II (1 μM) alone, Ang II (1 μM)/puerarin (100 μM) or puerarin alone (100 μM) for 24 hours before the cells were harvested for analysis.

2.7. Nrf2 siRNA transfection

For Nrf2-siRNA transfection, the cardiomyocytes were transfected with Nrf2-siRNA or Nrf2-negative control siRNA (Tab. S2, Viewsolid Biotech, Beijing, China) for 48 h upon plating the cells in a 6-well plate or 60 mm dish. The transfected cells were treated with Ang II (1 μM) alone, Ang II (1 μM)/puerarin (100 μM) or puerarin alone

(100 μM) for 24 h followed by further analysis.

2.8. Cell surface area measurement

The images of treated cardiomyocytes were obtained using a high-power microscope (Nikon Eclipse TS 100; Japan). The surface area was determined with NIH Image J software. Results were calculated based on 100 cells randomly selected from five wells for each group.

2.9. RNA isolation, quantitative RT-PCR

Total RNA was isolated using TRIzol reagent (Life Technologies, Grand Island, NY) from the left ventricular tissue or treated cardiomyocytes. Complementary DNA (cDNA) was synthesized using the First-Strand cDNA Synthesis Kit (Life Technologies, Grand Island, NY) following the manufacturer's instructions. Real-time PCR was performed using a QuantiTect SYBR Green PCR Kit (Takara Bio Inc., Japan) on an ABI StepOneTM Real-Time PCR system (Thermo Fisher Scientific Inc., California, USA). The sequences of the primer pairs for each gene are shown in Tab. S2. The GAPDH was used as normalization for qPCR

2.10. Western blot analysis

Whole protein extraction was prepared from left ventricular tissue or treated cardiomyocytes using RIPA buffer with protease and phosphatase inhibitors (BestBio Co., Shanghai, China). The proteins from the nucleus and cytoplasm were prepared

using the NE-PER® nuclear and cytoplasmic extraction kit (Thermo Fisher Scientific, Rockford, IL) following the manufacturer's protocol. Protein concentrations were quantified using the BCA kit (Thermo Fisher Scientific, USA). Equal protein amounts were resolved on 10% sodium dodecyl sulfate polyacrylamide gel electrophoresis and transferred to polyvinylidene difluoride membranes. The membrane was blocked with 5% no-fat milk in Tris-buffered saline 0.1% Tween-20 for 1 hour and then incubated with interested primary antibodies (all antibodies are shown in Tab. S1) at 4℃ overnight. The blot was then incubated with peroxidase-conjugated secondary antibody (ImmunoWay Biotechnology Co, USA) for 1 hour at room temperature. Bands of the proteins were observed using SuperSignal™ West Pico Chemiluminescent Substrate (Thermo, Rockford, IL, USA), and quantified analyses were performed with densitometry using NIH Image J software.

2.11. Immunofluorescence of cardiomyocytes

The treated cardiomyocytes were fixed with 4% paraformaldehyde for 10 min and permeabilized with 0.05% Triton X-100 for 15 min. The non-specific binding sites were blocked for 1 hour with 5% BSA in PBS. The cells were then incubated with NRF2 antibody (1:200) overnight followed by immunostaining with Dylight 488 anti-rabbit antibody (Thermo Fisher Scientific, USA) for 1 hour at room temperature. Nuclear counterstaining was performed with 4', 6-Diamidino-2-Phenylindole (DAPI, Sigma-Aldrich, St. Louis, MO). Coverslips were mounted on slides, and images were captured with a fluorescence microscope (Nikon Eclipse Ni-u; Japan) using

NIS-Elements software.

2.12. Chromatin Immunoprecipitation assay

A ChIP assay was performed with a ChIP assay kit (EZ-ChIP™, Catalog # 17-371, Thermo Fisher Scientific, USA) according to the manufacturer's instruction. Briefly, cardiomyocytes were incubated with 1% formaldehyde to crosslink the proteins to the DNA. Sonication is performed to shear the chromatin to a 200-1000 bp of DNA. The size of the DNA was verified by agarose gel electrophoresis. For the immunoprecipitation step, the primary antibody of NRF2 (1:100, CST) was used followed by protein G conjugated agarose beads to mutually enrich the protein and DNA complexes. Immunoprecipitated chromatins were incubated at 65 ℃ in 5M NaCl overnight to reverse cross-links. After digestion with proteinase K, DNA was recovered by phenol/chloroform extraction and ethanol precipitation. Precipitated DNA was analyzed by real-time PCR with the primers listed in Tab. S2.

2.13. Statistical analysis

Data were presented as the means ± standard error. Statistical analysis was performed with SPSS 18.0 software (IBM Corporation, Armonk, NY). The statistical differences between the groups were analyzed by one-way ANOVA followed by a post hoc Tukey test. $P<0.05$ was considered to be statistically significant.

JPET Fast Forward. Published on June 26, 2018 as DOI: 10.1124/jpet.118.248369
This article has not been copyedited and formatted. The final version may differ from this version.

3. Results

3.1. Puerarin attenuated AAC-induced cardiac hypertrophy

Using a rat model of AAC-induced cardiac hypertrophy, we evaluated whether puerarin may attenuate cardiac hypertrophy and ventricular remodeling at a dose of 50 mg/kg/d administered from 1 week after the surgery. Approximately 10% of the rats died within 24 hours after surgery; however, no more deaths were detected during the subsequent 7 weeks of the experiment, which indicates at least 8 rats for each group at the end of the study. Increased cardiac mass (Fig. 1A), myocyte cross sectional area (Fig. 1B), heart weight/body weight (HW/BW) ratio, and heart weight/tibial length (HW/TL) ratio (Fig. 1E) were observed in the rats subjected to AAC surgery after 7 weeks compared with the sham group, suggesting the exhibition of cardiac hypertrophy in the AAC group. Interestingly, injection with puerarin for six weeks significantly attenuated the above hypertrophic manifestations (Fig.1A, 1B and 1E). We further examined the expression of hypertrophic genes. As shown in Fig. 1F, the mRNA expression of atrial natriuretic peptide (*ANP*) and beta myosin heavy chain (*Myh7*), which were upregulated after ACC surgery, were significantly blunted in the puerarin injection rats. A key feature of cardiac hypertrophy and remodeling is myocardial fibrosis. Therefore, Masson trichrome and PSR staining on cardiac tissue sections were performed to evaluate the severity of myocardial interstitial and perivascular fibrosis in each group. As shown in Fig. 1C and 1D, interstitial and

perivascular fibrosis were remarkable after 7 weeks of AAC, which were ameliorated by puerarin administration. The protective effect of puerarin on cardiac hypertrophy induced by AAC was evaluated by echocardiograph. As shown in Fig. 2, 7 weeks after ACC surgery, hypertrophic indicators such as left ventricular posterior wall diameter (LVPWd) and intraventricular septum diameter (IVSd) increased significantly in the AAC group compared to the sham group (Fig. 2A to 2C). Conversely, left ventricular internal diameter (LVId) decreased (Fig. 2D) in rats with AAC surgery. Puerarin administration resulted in a significant reversal of these hypertrophic indicators (Fig. 2A-2D). The left ventricular ejection fraction (LVEF) and left ventricular fractional shortening (LVFS) did not show significant changes in each group at the end of this study (Fig. 2E).

3.2. Puerarin improved AAC-induced hemodynamic parameters

Catheter-based hemodynamic measurements were performed at the end of the study to further detect the changes of left ventricular systolic and diastolic function. As shown in Table 1, 7 weeks of AAC resulted in significantly increased systolic blood pressure, diastolic blood pressure and left ventricular end-systolic pressure (LVESP). Puerarin administration normalized these hemodynamic parameters. However, the parameters including left ventricular end-diastolic pressure (LVEDP), Max +dP/dt and Max -dp/dt were not significantly different between the groups.

3.3. Puerarin protected against cardiac hypertrophy and oxidative stress via the

JPET Fast Forward. Published on June 26, 2018 as DOI: 10.1124/jpet.118.248369
This article has not been copyedited and formatted. The final version may differ from this version.

activation of Nrf2 in vivo

Nrf2 is the master regulator of the antioxidant response. Kelch-Like ECH-Associated Protein 1 (Keap1) is an E3 ubiquitin ligase substrate adaptor, and regulates the level of Nrf2 protein in a redox-dependent fashion. Stress-related modification of Keap1 results in Nrf2 stabilization, accumulation of the transcription factor in the nucleus, where Nrf2 binds to the antioxidant/electrophile-response element (ARE) and protects against oxidative stress damage (Rada et al., 2011). To assess whether puerarin can activate the Nrf2-Keap1 pathway in rats with AAC surgery, we evaluated the transcription of *Nrf2* mRNA by RT-PCR and the protein expression of NRF2 by Western blotting in liver and heart tissues from each group (Fig 3). Although NRF2 protein expression did not show a significant difference between the sham group and AAC group in rat livers, its mRNA and protein levels were significantly decreased in AAC hearts compared with the control. Moreover, puerarin treatment significantly increased the Nrf2 mRNA and protein levels in the hearts and livers from the AAC and sham rats, accompanied by decreased KEAP1 protein (Fig. 3A-3D). Because NRF2 accumulation in nucleus may indicate its activation, we further detected its protein expression in the nuclear and cytoplasmic fractions of heart lysates. As shown in Fig. 3E, compared with the sham group, rats from the AAC surgery groups exhibited significantly decreased translocation of NRF2 from the cytosol to the nuclear fraction. In contrast, puerarin significantly enhanced its nucleus accumulation. The cytosolic NRF2 level was not significant different between the groups. Immunohistochemical staining also showed an increment in nuclear NRF2 but a

reduction in nuclear KEAP1 in AAC-Pue rats compared with AAC rats (Fig. 3G, 3H). We further measured the protein levels of heme oxygenase 1 (HO1), glutathione transferase p1 (GSTP1) and NAD(P)H:quinone oxidoreductase 1 (NQO1), which are well-known downstream antioxidant proteins of Nrf2. The expression of HO1, GSTP1 and NQO1 was decreased in rats with AAC surgery compared with those in the sham group. The difference in GSTP1 and NQO1 were statistically significant. However, puerarin remarkably increased their protein levels in both AAC-Pue and sham-Pue rats (Fig. 3F).

3.4. Puerarin induced Nrf2 nuclear translocation in AngII-induced cardiomyocytes hypertrophy

To further determine whether puerarin could activate Nrf2 in the pathophysiological process of cardiac hypertrophy, we examined its effects on hypertrophic changes in NRCMs due to Ang II. Treatment with Ang II (1 μM) resulted in a significantly increased cell surface area (Fig. 4A and 4B, $P<0.05$) and upregulated the mRNA levels of *ANP* and *Myh7* (Fig. 4C). More importantly, these hypertrophic changes were attenuated by co-incubation with puerarin (100 μM, Fig. 4A-4C). We further evaluated the NRF2 and KEAP1 protein levels using Western blotting. As shown in Fig. 4D, the NRF2 protein levels were significantly higher in the overall and nuclear lysates from cardiomyocytes treated with puerarin alone than control cells. Reduced NRF2 and increased KEAP1 were observed in Ang II-treated cardiomyocytes, which were reversed by puerarin treatment. Moreover, Ang II significantly decreased the

translocation of NRF2 from the cytosol to the nucleus. Co-incubation with puerarin restored the NRF2 activity induced by Ang II (Fig. 4E). Immunofluorescence staining also revealed that NRF2 accumulated in the nuclei of cardiomyocytes treated with Ang II and puerarin or puerarin alone (Fig. 4F).

3.5. Puerarin protected against Ang II-induced cardiomyocyte hypertrophy and oxidative stress through the activation of Nrf2

The role of Nrf2 in puerarin's anti-hypertrophy property was further confirmed via siRNA. After transfection with Nrf2 siRNA or negative control siRNA for 48 hours, cardiomyocytes were subsequently treated with Ang II (1 μM) alone, in combination with Ang II (1 μM) and puerarin (100 μM), or puerarin alone (100 μM) for another 24 hours. Fig. 5C and 5D demonstrated that using Nrf2 siRNA dramatically inhibited Nrf2 mRNA and protein expression compared with the negative control. Moreover, Nrf2 siRNA attenuated the anti-hypertrophic effects of puerarin. The puerarin-induced upregulation of hypertrophic indicators, such as cell surface area and hypertrophic genes, were also partially abolished with the silencing of Nrf2 expression with specific siRNA (Fig. 5A-5C). In addition, we also evaluated the expression of HO1, GSTP1 and NQO1. Similar to the rats in the AAC group, Ang II treatment decreased the expression of the antioxidant proteins, which was blocked by puerarin treatment (Fig. 5D and 5E). The puerarin-induced anti oxidative effect was abolished by silencing Nrf2 expression with specific siRNA (Fig. 5D and 5E). These data further supported that the puerarin-induced cardiac protection was partially mediated through

transcription activator Nrf2.

3.6. Puerarin upregulated the expression of the drug-metabolizing enzymes UGT1A1 and UGT1A9

Glucuronidation represents a major conjugative reaction catalyzed by UDP-glucuronosyltransferases (UGTs). According to our previous results, UGT1A1, 1A9 significantly catalyzed the formation of puerarin metabolites, and the activity of UGT1A1 was significantly higher than that of other enzymes (Luo et al., 2012). We detected UGT1A1 and 1A9 expression using RT-PCR and Western blotting in the liver and heart tissues from the rats in each group. Fig 6. shows that the mRNA and protein levels of UGT1A1 and UGT1A9 were significantly increased in the livers and hearts from rats of AAC-puerarin and Sham-puerarin groups compared with their controls. The expression of these two metabolic enzymes was not significantly different in the AAC rats compared with the Sham group (Fig. 6A-6F). Immunohistochemical staining also indicated that UGT1A1 and UGT1A9 increased in the puerarin administration groups (Fig. 6G, 6H).

3.7. Puerarin upregulated UGT1A1 and UGT1A9 levels through the activation of Nrf2 in cardiomyocytes

A majority of reports have indicated that Nrf2 may be an important regulator of the *Ugt1as* gene (Kundu et al., 2011); thus, we further identified the role of Nrf2 in puerarin-stimulated UGT1A1 and UGT1A9 upregulation with Nrf2 siRNA in

AngII-treated cardiomyocytes. Although the mRNA and protein levels of UGT1A1 and UGT1A9 in AngII-treated cardiomyocytes were not significantly different, they were significantly induced after incubation with puerarin for 24 hours compared with the control cells. Moreover, after the specific down-regulation of Nrf2 with siRNA, the puerarin-induced upregulation of UGT1A1 and UGT1A9 was partially abolished (Fig. 7A, 7B). These data suggested that Nrf2 activation played a pivotal role in the puerarin-induced expressions of UGT1A1 and UGT1A9.

3.8. Puerarin-induced Nrf2 upregulation is relative to elevated UGT1A1 and UGT1A9 promoter activation

To demonstrate that Nrf2 may induce the transcription of UGT1A1 or UGT1A9 by binding to the promoters of the genes, we performed ChIP-qPCR in control and puerarin-treated cardiomyocytes. Each IP was immunoprecipitated with anti-Nrf2 antibody. We found that puerarin significantly enhanced the binding of Nrf2 to the *Ugt1a1* or *Ugt1a9* promoter region observed in puerarin-treated cardiomyocytes compared with control cells and negative controls (Fig. 8D, 8E).

4. Discussion

We and others reported that puerarin can prevent the cardiac hypertrophy induced by pressure overload (Chen et al., 2014; Yuan et al., 2014; Chen et al., 2015; Liu et al., 2015; Zhang et al., 2016). Similarly, the present study indicated that puerarin could

inhibit AAC-induced cardiac hypertrophy in rats and Ang II-induced cardiomyocytes. These results suggest that the benefits of puerarin for the cardiovascular system may at least partially depend on its attenuation of cardiac hypertrophy and ventricular remodeling.

Nrf2 is a member of the cap-n-collar family of transcription factors. Keap1 is a specific regulator of Nrf2(Kensler et al., 2007). Accumulation of Nrf2 in the nucleus leads to its binding to ARE in the upstream promoter region, and promotes the transcription of a battery of antioxidative genes, including *Ho1, Nqo1, Gstp1*, and others (Kensler et al., 2007; Zhou et al., 2014a; Taguchi et al., 2016). It has recently been reported that pharmacological activation of Nrf2 can reverse liver fibrosis in a mouse model of non-alcoholic steatohepatitis (Sharma et al., 2018). The Nrf2-mediated pathway has been reported to play an important role in cardiac hypertrophy and remodeling (Zhou et al., 2014a). *Nrf2* knockout mice undergo cardiac hypertrophy and progress to heart failure (Erkens et al., 2015; Strom and Chen, 2017). The activation of Nrf2 regulates redox homeostasis (Jung and Kwak, 2010) and suppresses inflammation (Qu et al., 2015) and endoplasmic reticulum stress (Cominacini et al., 2015). These are involved in the pathogenesis of cardiac hypertrophy (Cominacini et al., 2015; Tham et al., 2015). Accumulating data suggested that oxidative stress is an important mechanism involved in the development of cardiac hypertrophy (Tham et al., 2015). We showed that puerarin could protect against cardiomyocyte hypertrophy induced by Ang II via inhibiting

JPET Fast Forward. Published on June 26, 2018 as DOI: 10.1124/jpet.118.248369
This article has not been copyedited and formatted. The final version may differ from this version.

oxidative stress in neonatal rat cardiomyocytes (Hou et al., 2017).These results were further confirmed by current findings that puerarin significantly increased the expression of Nrf2 in the hearts of pressure-overload rats and NRCMs treated by Ang II. Puerarin treatment also decreased the protein level of Keap1 in the hearts of pressure-overload rats and NRCMs treated by Ang II. Additionally, the level of Nrf2 protein in the nucleus was significantly increased in both hearts and NRCMs, although the level of Nrf2 protein in cytosol remained similar. The upregulation of nuclear Nrf2 enhanced the expression of HO1, NQO1, and GSTP1 in the myocardium of pressure-overload rats and NRCMs treated by Ang II. The down-regulation of Nrf2 by siNrf2 could inhibit the increase of these antioxidative genes induced by puerarin in NRCMs treated with Ang II, and the antihypertrophic efficacy of puerarin was also simultaneously suppressed. These results indicated that puerarin could prevent cardiac hypertrophy via Nrf2-mediated antioxidative mechanisms.

Besides Keap1, Nrf2 is negatively regulated by another ubiquitin ligase substrate adaptor, β-transducin repeat-containing protein (β-TrCP). Keap1 and β-TrCP respectively allow cullin-3 and cullin-1 to ubiquitylate Nrf2. In the case of Keap1, thiol-reactive electrophiles cause inactivation of its adaptor function by modifying Cys residues and this blunts ubiquitylation of Nrf2. In the case of β-TrCP, it recognizes a DSGIS-containing phosphodegron in Nrf2 that is formed by glycogen synthase kinase-3 (GSK-3). Thus, when Nrf2 is phosphorylated by GSK-3, the binding of β-TrCP to Nrf2 then enables cullin-1 to ubiquitylate Nrf2 that leads to

proteasomal degradation of the transcription factor (Rada et al., 2011; Chowdhry et al., 2013). Using Keap1-null MEFs, it has been shown that a variety of phytochemical inducers can activate Nrf2 in a Keap1-independent manner, presumably by inactivating GSK-3 directly, increasing the inhibitory phosphorylation of Ser-9/21 in GSK-3, or by preventing it from phosphorylating Nrf2 (Hayes et al., 2016). It has been reported previously that puerarin exerts hepatoprotective effects via down-regulating GSK-3β(Katsiki et al., 2013). It therefore seems likely that puerarin may inactivate GSK-3 or inhibit a priming kinase.

Transcription factors, including AhR, CAR, and PXR, are important regulators for the expression of drug-metabolizing enzymes. Intriguingly, feedback loops are generated when activators of the transcription factor are substrates of drug-metabolizing enzymes, which are regulated by the transcription factors, and this has been proposed as an important mechanism for maintaining homeostasis in drug-metabolizing enzymes (Bock, 2012; Bock, 2014). Previous evidence suggests that Nrf2 may be a key transcription factor regulating the expression of genes for xenobiotic metabolism(Kensler et al., 2007). Nrf2 has been reported to up-regulate the expression of UGT1A1 and UGT1A6 (Thimmulappa et al., 2002; Kundu et al., 2011; Bai et al., 2016). In our study, UGT1A1 and UGT1A9 mRNA and protein were detected in the livers and hearts of rats, as well as in NRCMs. In liver and heart tissues of rats after 7 weeks of AAC, puerarin significantly increased the mRNA and protein levels of UGT1A1 and UGT1A9. In NRCMs treated by Ang II, the mRNA

and protein levels of UGT1A1 and UGT1A9 were also upregulated by puerarin. The down-regulation of Nrf2 by siNrf2 inhibited the upregulation of UGT1A1 and 1A9 protein levels induced by puerarin in Ang II-treated NRCMs. Taken together, these results suggest that puerarin may induce its metabolic enzymes UGT1A1 and 1A9 expression via Nrf2. ChIP assay results further confirmed that puerarin enhanced the binding of Nrf2 to the UGT1A1 and 1A9 promoter in NRCMs.

This autoregulatory circuit between puerarin and its metabolic enzymes may be similar to the mechanisms underlying the metabolism of other biological compounds. In the early 1980, Boutin and colleagues (Boutin et al., 1983) reported that xenobiotics, such as eugenol and 4-methylumbelliferone, induce UGT activity and enhance their own conjugation. Flavone compounds have been reported to increase the expression and activity of UGT1A1 in some cell lines (Galijatovic et al., 2000; Walle et al., 2000; Kundu et al., 2011). Similarly, bilirubin is an activator of AhR (Togawa et al., 2008) and CAR (Huang et al., 2003). Bilirubin subsequently induces the expression of UGT1A1 and enhances the clearance of bilirubin, which indicates that the feedback loops between bilirubin and AhR/CAR-induced UGT1A1 are useful to maintain the homeostasis of bilirubin. Similar autoregulatory circuits were also demonstrated between quercetin and AhR/Nrf2-regulated UGT1A1 (Bock, 2012). Our results suggested that there may be an autoregulatory circuit between puerarin and Nrf2-regulated UGT1A1/1A9.

It is very important to maintain the homeostasis of metabolizing enzymes of puerarin because the intravenous administration of puerarin has been associated with severe side effects, such as intravascular hemolysis. The mechanism for the development of intravascular hemolysis remains uncertain, which may be associated with changes in membrane lipids and the composition of erythrocyte membrane proteins after incubation with puerarin *in vitro*, perhaps in a concentration-dependent manner (Hou et al., 2011). After puerarin administration, the upregulation of UGT1A1 and UGT1A9 will enhance puerarin metabolism. From our point of view, this will have at least two effects. Firstly, the concentration of puerarin in the plasma will decrease, which may be an initial protective effect for the incidence of severe side effects, such as intravascular hemolysis. Secondly, the metabolites of puerarin will increase, including puerarin-7-*O*-glucuronide. Our previous study suggested that puerarin-7-*O*-glucuronide can exert antioxidative and antihypertrophic efficacy in cardiomyocytes (Hou et al., 2017), which indicates that the upregulation of UGT1A1 and UGT1A9 induced by puerarin may decrease the risk of severe side effects without significantly changing antihypertrophic effects as compensated by the antihypertrophic efficacy of its metabolites. Interestingly, Nrf2 appears to be an important transcription factor not only underlying the preventative efficacy of puerarin against cardiac hypertrophy but also in upregulating the metabolizing enzymes of puerarin.

In conclusion, puerarin can enhance the expression of transcription factor Nrf2 and its

JPET Fast Forward. Published on June 26, 2018 as DOI: 10.1124/jpet.118.248369
This article has not been copyedited and formatted. The final version may differ from this version.

translocation into the nucleus. On the one hand, the upregulation and translocation of Nrf2 can promote the expression of antioxidative genes and prevent cardiac hypertrophy. On the other hand, the upregulation and translocation of Nrf2 can increase the expression of metabolizing enzymes of puerarin, including UGT1A1 and UGT1A9. These dual effects of transcription factor Nrf2 and potential autoregulatory circuits between puerarin and Nrf2-regulated UGT1A1/1A9 may be important to maintain antihypertrophic efficacy and to limit the risk of the potential side effects of puerarin.

Conflict of interest

The authors declare no conflicts of interest.

Authorship Contributions

Participated in research design: GJZ, NH, SAC, XWL, CFL and MSC

Conducted experiments: GJZ, NH, SAC, XWL, AQL,CFC, YH and LRL

Supervised experiments: CFL and MSC

Contributed new reagents or analytic tools: CWO,YPM and ZYX

Performed data analysis: GJZ, NH, SAC and XWL

Wrote or contributed to the writing of the manuscript: GJZ, NH, SAC, XWL and CFL

Revisions and submission considerations: SML, XHC and MSC

References

Bai X, Chen Y, Hou X, Huang M and Jin J (2016) Emerging role of NRF2 in chemoresistance by regulating drug-metabolizing enzymes and efflux transporters. *Drug Metab Rev* **48**:541-567.

Bock KW (2012) Human UDP-glucuronosyltransferases: Feedback loops between substrates and ligands of their transcription factors. *Biochem Pharmacol* **84**:1000-1006.

Bock KW (2014) Homeostatic control of xeno- and endobiotics in the drug-metabolizing enzyme system. *Biochem Pharmacol* **90**:1-6.

Boutin JA, Batt AM and Siest G (1983) Effect of pretreatment with hydroxylated xenobiotics on the activities of rat liver UDP-glucuronosyl-transferases. *Xenobiotica* **13**:755-761.

Chen G, Cao Q, Cui X, Pan S, Shen C and Liu L (2015) Puerarin suppresses angiotensin II-induced cardiac hypertrophy by inhibiting NADPH oxidase activation and oxidative stress-triggered AP-1 signaling pathways. *J Pharm Pharm Sci* **18**:235-248.

Chen G, Pan S-Q, Shen C, Pan S-F, Zhang X-M and He Q-Y (2014) Puerarin inhibits angiotensin II-induced cardiac hypertrophy via the redox-sensitive ERK1/2, p38 and NF-kappa B pathways. *Acta Pharmacol Sin* **35**:463-475.

Chowdhry S, Zhang Y, McMahon M, Sutherland C, Cuadrado A and Hayes JD (2013) Nrf2 is controlled by two distinct beta-TrCP recognition motifs in its Neh6 domain, one of which can be modulated by GSK-3 activity. *Oncogene* **32**:3765-3781.

Cominacini L, Mozzini C, Garbin U, Pasini A, Stranieri C, Solani E, Vallerio P, Tinelli IA and Fratta Pasini A (2015) Endoplasmic reticulum stress and Nrf2 signaling in cardiovascular diseases. *Free Radic Biol Med* **88**:233-242.

Erkens R, Kramer CM, Lueckstaedt W, Panknin C, Krause L, Weidenbach M, Dirzka J, Krenz T, Mergia E, Suvorava T, Kelm M and Cortese-Krott MM (2015) Left ventricular diastolic dysfunction in Nrf2 knock out mice is associated with cardiac hypertrophy, decreased expression of SERCA2a, and preserved endothelial function. *Free Radic Biol Med* **89**:906-917.

Galijatovic A, Walle UK and Walle T (2000) Induction of UDP-glucuronosyltransferase by the flavonoids chrysin and quercetin in Caco-2 cells. *Pharm Res* **17**:21-26.

Gao L, Ji X, Song J, Liu P, Yan F, Gong W, Dang S and Luo Y (2009) Puerarin protects against ischemic brain injury in a rat model of transient focal ischemia. *Neurol Res* **31**:402-406.

Hayes JD, Ebisine K, Sharma RS, Chowdhry S, Dinkova-Kostova AT and Sutherland C (2016) Regulation of the CNC-bZIP transcription factor Nrf2 by Keap1 and the axis between GSK-3 and β-TrCP. *Curr Opin Toxicol* **1**:92-103.

Hou N, Cai B, Ou CW, Zhang ZH, Liu XW, Yuan M, Zhao GJ, Liu SM, Xiong LG, Luo JD, Luo CF and Chen MS (2017) Puerarin-7-*O*-glucuronide, a water-soluble puerarin metabolite, prevents angiotensin II-induced cardiomyocyte hypertrophy by reducing oxidative stress. *Naunyn Schmiedebergs Arch Pharmacol* **390**:535-545.

Hou SZ, Su ZR, Chen SX, Ye MR, Huang S, Liu L, Zhou H and Lai XP (2011) Role of the interaction between puerarin and the erythrocyte membrane in puerarin-induced hemolysis. *Chem Biol Interact* **192**:184-192.

Hsu FL, Liu IM, Kuo DH, Chen WC, Su HC and Cheng JT (2003) Antihyperglycemic effect of puerarin in streptozotocin-induced diabetic rats. *J Nat Prod* **66**:788-792.

Huang J, Tang X, Liang X, Wen Q, Zhang S, Xuan F, Jian J, Lin X and Huang R (2015) The Effects of 17-methoxyl-7-hydroxy-benzene-furanchalcone on pressure overload-induced cardiac remodeling in rats and the endothelial mechanisms based on PGI(2). *Cell Physiol Biochem* **36**:1004-1014.

Huang W, Zhang J, Chua SS, Qatanani M, Han Y, Granata R and Moore DD (2003) Induction of bilirubin clearance by the constitutive androstane receptor (CAR). *Proc Natl Acad Sci U S A* **100**:4156-4161.

Jung KA and Kwak MK (2010) The Nrf2 system as a potential target for the development of indirect antioxidants. *Molecules* **15**:7266-7291.

Kamo T, Akazawa H and Komuro I (2015) Cardiac Nonmyocytes in the Hub of Cardiac Hypertrophy. *Circ Res* **117**:89-98.

Katsiki N, Karagiannis A and Mikhailidis DP (2013) Diabetes, bilirubin and amputations: is there a link? *Diabetologia* **56**:683-685.

Kensler TW, Wakabayash N and Biswal S (2007) Cell survival responses to environmental stresses via the Keap1-Nrf2-ARE pathway. *Annu Rev Pharmacol Toxicol* **47**:89-116.

Ku H, Lee S, Wu YA, Yang K and Su M (2016) A model of cardiac remodeling through constriction of the abdominal aorta in rats. *J Vis Exp*: doi: 10.3791/54818.

Kundu R, Dasgupta S, Biswas A, Bhattacharya S, Pal BC, Bhattacharya S, Rao PG, Barua NC, Bordoloi M and Bhattacharya S (2011) Carlinoside reduces hepatic bilirubin accumulation by stimulating bilirubin-UGT activity through Nrf2 gene expression. *Biochem Pharmacol* **82**:1186-1197.

Li H, Dong L, Liu Y, Wang G and Qiao Y (2014) Biopharmaceutics classification of puerarin and comparison of perfusion approaches in rats. *Int J Pharm* **466**:133-138.

Liu B, Wu Z, Li Y, Ou C, Huang Z, Zhang J, Liu P, Luo C and Chen M (2015) Puerarin prevents cardiac hypertrophy induced by pressure overload through activation of autophagy. *Biochem Biophys Res Commun* **464**:908-915.

Luo CF, Cai B, Hou N, Yuan M, Liu SM, Ji H, Xiong LG, Xiong W, Luo JD and Chen MS (2012) UDP-glucuronosyltransferase 1A1 is the principal enzyme responsible for puerarin metabolism in human liver microsomes. *Arch Toxicol* **86**:1681-1690.

Luo CF, Hou N, Tian J, Yuan M, Liu SM, Xiong LG, Luo JD and Chen MS (2013) Metabolic profile of puerarin in rats after intragastric administration of puerarin solid lipid nanoparticles. *Int J Nanomedicine* **8**:933-940.

Luo CF, Yuan M, Chen MS, Liu SM, Huang BY, Liu XW and Zhu L (2011a) Determination of puerarin in rat plasma by rapid resolution liquid chromatography tandem mass spectrometry in positive ionization mode. *J Chromatogr B Analyt Technol Biomed Life Sci* **879**:1497-1501.

Luo CF, Yuan M, Chen MS, Liu SM, Zhu L, Huang BY, Liu XW and Xiong W (2011b) Pharmacokinetics, tissue distribution and relative bioavailability of puerarin solid lipid nanoparticles following oral administration. *Int J Pharm* **410**:138-144.

Mackenzie PI, Hu DG and Gardner-Stephen DA (2010) The regulation of UDP-glucuronosyltransferase genes by tissue-specific and ligand-activated transcription factors. *Drug Metab Rev* **42**:99-109.

Oka T, Akazawa H, Naito AT and Komuro I (2014) Angiogenesis and Cardiac Hypertrophy Maintenance of Cardiac Function and Causative Roles in Heart Failure. *Circ Res* **114**:565-571.

Qu C, Li B, Lai Y, Li H, Windust A, Hofseth LJ, Nagarkatti M, Nagarkatti P, Wang XL, Tang D, Janicki JS, Tian X and Cui T (2015) Identifying panaxynol, a natural activator of nuclear factor erythroid-2

related factor 2 (Nrf2) from American ginseng as a suppressor of inflamed macrophage-induced cardiomyocyte hypertrophy. *J Ethnopharmacol* **168**:326-336.

Rada P, Rojo AI, Chowdhry S, McMahon M, Hayes JD and Cuadrado A (2011) SCF/β-TrCP promotes glycogen synthase kinase 3-dependent degradation of the Nrf2 transcription factor in a Keap1-independent manner. *Mol Cell Biol* **31**:1121-1133.

Reddy DS, Singh M, Ghosh S and Ganguly NK (1996) Role of cardiac renin-angiotensin system in the development of pressure-overload left ventricular hypertrophy in rats with abdominal aortic constriction. *Mol Cell Biochem* **155**:1-11.

Sharma RS, Harrison DJ, Kisielewski D, Cassidy DM, McNeilly AD, Gallagher JR, Walsh SV, Honda T, McCrimmon RJ, Dinkova-Kostova AT, Ashford MLJ, Dillon JF and Hayes JD (2018) Experimental Nonalcoholic Steatohepatitis and Liver Fibrosis Are Ameliorated by Pharmacologic Activation of Nrf2 (NF-E2 p45-Related Factor 2). *Cellular and molecular gastroenterology and hepatology* **5**:367-398.

Simpson P and Savion S (1982) Differentiation of rat myocytes in single cell cultures with and without proliferating nonmyocardial cells. Cross-striations, ultrastructure, and chronotropic response to isoproterenol. *Circ Res* **50**:101-116.

Song XP, Chen PP and Chai XS (1988) Effects of puerarin on blood pressure and plasma renin activity in spontaneously hypertensive rats. *Zhongguo Yao Li Xue Bao* **9**:55-58.

Strom J and Chen QM (2017) Loss of Nrf2 promotes rapid progression to heart failure following myocardial infarction. *Toxicol Appl Pharmacol* **327**:52-58.

Sugatani J, Nishitani S, Yamakawa K, Yoshinari K, Sueyoshi T, Negishi M and Miwa M (2005) Transcriptional regulation of human UGT1A1 gene expression: activated glucocorticoid receptor enhances constitutive androstane receptor/pregnane X receptor-mediated UDP-glucuronosyltransferase 1A1 regulation with glucocorticoid receptor-interacting protein 1. *Mol Pharmacol* **67**:845-855.

Taguchi K, Takaku M, Egner PA, Morita M, Kaneko T, Mashimo T, Kensler TW and Yamamoto M (2016) Generation of a new model rat: Nrf2 knockout rats are sensitive to aflatoxin B1 toxicity. *Toxicol Sci* **152**:40-52.

Tham YK, Bernardo BC, Ooi JYY, Weeks KL and McMullen JR (2015) Pathophysiology of cardiac hypertrophy and heart failure: signaling pathways and novel therapeutic targets. *Arch Toxicol* **89**:1401-1438.

Thimmulappa RK, Mai KH, Srisuma S, Kensler TW, Yamamoto M and Biswal S (2002) Identification of Nrf2-regulated genes induced by the chemopreventive agent sulforaphane by oligonucleotide microarray. *Cancer Res* **62**:5196-5203.

Togawa H, Shinkai S and Mizutani T (2008) Induction of human UGT1A1 by bilirubin through AhR dependent pathway. *Drug Metab Lett* **2**:231-237.

Walle T, Otake Y, Galijatovic A, Ritter JK and Walle UK (2000) Induction of UDP-glucuronosyltransferase UGT1A1 by the flavonoid chrysin in the human hepatoma cell line hep G2. *Drug Metab Dispos* **28**:1077-1082.

Yan LP, Chan SW, Chan ASC, Chen SL, Ma XJ and Xu HX (2006) Puerarin decreases serum total cholesterol and enhances thoracic aorta endothelial nitric oxide synthase expression in diet-induced hypercholesterolemic rats. *Life Sci* **79**:324-330.

Yuan Y, Zong J, Zhou H, Bian ZY, Deng W, Dai J, Gan HW, Yang Z, Li H and Tang QZ (2014) Puerarin attenuates pressure overload-induced cardiac hypertrophy. *J Cardiol* **63**:73-81.

Zhang S, Chen S, Shen Y, Yang D, Liu X, Sun-Chi AC and Xu H (2006) Puerarin induces angiogenesis in myocardium of rat with myocardial infarction. *Biol Pharm Bull* **29**:945-950.

Zhang X, Liu Y and Han Q (2016) Puerarin attenuates cardiac hypertrophy partly through increasing Mir-15b/195 expression and suppressing non-canonical transforming growth factor Beta (Tgf beta) signal pathway. *Med Sci Monit* **22**:1516-1523.

Zhou S, Sun W, Zhang Z and Zheng Y (2014a) The role of Nrf2-mediated pathway in cardiac remodeling and heart failure. *Oxid Med Cell Longev* **2014**:260429-260429.

Zhou YX, Zhang H and Peng C (2014b) Puerarin: A Review of Pharmacological Effects. *Phytother Res* **28**:961-975.

Footnotes

This work was supported by the National Natural Science Foundation of China [grant numbers 81374009, U1501222, 81402928], Guangdong Natural Science Foundation [grant number 2014A030313493], Guangzhou Education Bureau [grant number 2012C090], and The Key Medical Disciplines and Specialties Program of Guangzhou [2017-2019].

[1] Gan-Jian Zhao, Ning Hou, Shao-Ai Cai, and Xia-Wen Liu contributed equally to this work.

Legends for Figures

Fig. 1 Puerarin protected against abdominal aortic constriction (AAC)-induced cardiac hypertrophy. A: Gross hearts (upper); hematoxylin and eosin (H&E) staining for longitudinal section of rat heart (lower). B: H&E staining of sham and AAC hearts after 6 weeks puerarin treatment. The cross section of myocardium (upper). Perivascular cardiomyocytes (lower). C: Representative images of Masson trichrome staining for interstitial fibrosis of myocardium (upper) and perivascular fibrosis (lower). D: Picrosirius red staining indicated myocardial fibrosis representatively by upright microscopy (upper) and polarization microscope (lower). E: Heart weight/body weight (HW/BW) ratio and heart weight/tibial length (HW/TL) ratio. F: Reverse transcription-polymerase chain reaction analysis for atrial natriuretic peptide (*Anp*) and beta myosin heavy chain (*Myh7*) mRNA expression. AAC, abdominal aortic constriction group; AAC+Pue, puerarin injected-AAC group; Pue, puerarin injected-sham group. Representative images from 3 sets of staining are shown. * $P < 0.05$ vs. sham group; # $P < 0.05$ vs. AAC group, n=8 for each group. Each group contained equal numbers of male and female rats.

Fig.2 Puerarin improved AAC-induced cardiac hypertrophy as indicated by echocardiographic examinations. A: Representative M-mode images of the indicated groups. B, C and D: Parameters of cardiac structure. LVPWd, left ventricular posterior wall diameter; IVSd, interventricular septum diameter; LVId, left ventricular interior diameter. E: Left ventricular function changes in ejection fraction (LVEF) and

fractional shortening (LVFS). * $P < 0.05$ *vs*. sham group; # $P < 0.05$ *vs*. AAC group, n=8 for each group (4 male and 4 female rats).

Fig. 3 Puerarin protected against cardiac hypertrophy and oxidative stress through Nrf2 activation in pressure-overload hearts. A: Quantitative reverse transcription PCR analysis of *Nrf2* expression in the heart and liver. B and C: Representative Western blots of whole lysate and fold increases in relative densitometric values of NRF2 in hearts (B) and livers (C) from indicated groups. D: Representative Western blots of whole lysate and fold increases in relative densitometric values of KEAP1 in hearts. E: Representative Western blots and fold increases in relative densitometric values of NRF2 in the cytoplasmic, nuclear lysates from the indicated hearts. F: Representative Western blots and fold increases in the relative densitometric values of HO1, GSTP1, and NQO1 levels in hearts from each group. G: Representative images of immunohistochemical staining for NRF2 (upper) and KEAP1 (lower) expression in hearts from each group. Scale bar = 50 μm. H: Analysis of immunohistochemistry integrated optical density (IOD) values. * $P < 0.05$ *vs*. sham group; # $P < 0.05$ *vs*. AAC group, n=8 for each group. Each group included 4 male and 4 female rats.

Fig.4 Puerarin stimulated Nrf2 nucleus translocation in Ang II-induced neonatal rat cardiomyocytes (NRCMs) hypertrophy. A and B: Representative micrographs (A) and measurement of surface area (B) for cardiomyocytes subjected to different treatments as indicated. C: Reverse transcription-polymerase chain reaction analysis for atrial

natriuretic peptide (*Anp*) and beta myosin heavy chain (*Myh7*) in NRCMs subjected to indicate treatments. D: Representative Western blots of whole lysate and fold increases in relative densitometric values of NRF2 and KEAP1 in each group. E: Representative Western blots and fold increases in relative densitometric values of NRF2 in the cytoplasmic, nuclear lysates from the indicated groups. F: Representative immunofluorescence images demonstrating nuclear localization of NRF2 in cardiomyocytes. * $P < 0.05$ *vs*. control group; $^{\#}$ $P < 0.05$ *vs*. Ang II group, n=6 for each group.

Fig.5 Puerarin protected against Ang II-induced cardiomyocyte hypertrophy and oxidative stress through activation of Nrf2. A and B: Representative micrographs (A) and measurement of surface area (B) for cardiomyocytes subjected to different treatments as indicated. C and D: Reverse transcription-polymerase chain reaction analysis for *Anp*, *Myh7*(C) and *Nrf2*(D) in NRCMs subjected to indicated treatments. E and F: Representative Western blots of whole lysate (E) and fold changes (F) in relative densitometric values of NRF2, HO1, GSTP1, and NQO1 in cultured rat ventricular cardiomyocytes under different treatments. * $P < 0.05$ *vs*. Control + negative control (NC) siRNA group; $^{\#}$ $P < 0.05$ *vs*. AngII + negative control (NC) siRNA group, §$P < 0.05$ vs. AngII +Puerarin + negative control (NC) siRNA group, $^{\vartriangle}$ $P<0.05$ *vs*. Puerarin + negative control (NC) siRNA group, n=6 for each group.

Fig. 6 Puerarin upregulated the expression of drug-metabolizing enzymes UGT1A1

and UGT1A9. A and B: Representative Western blots of UGT1A1 and UGT1A9 in whole lysates and fold changes in relative densitometric values in rat hearts from each group. C: Fold changes in *Ugt1a1* and *1a9* mRNA levels by real-time RT-PCR in rat hearts from each group. D and E: Representative Western blots of UGT1A1 and UGT1A9 in whole lysates and fold changes in relative densitometric values in rat livers from each group. F: Fold changes in *Ugt1a1* and *1a9* mRNA levels by real-time RT-PCR in rat livers from each group. n=8 for each group (4 male and 4 female rats) . G: Representative images of immunohistochemical staining from 3 rat hearts in each group for UGT1A1 (upper) and 1A9 (lower). H: Quantitative integrated optical density (IOD) values of UGT1A1 and 1A9. * $P < 0.05$ *vs*. sham group; $^{\#}$ $P < 0.05$ *vs*. AAC group.

Fig. 7 Puerarin upregulated UGT1A1 and UGT1A9 levels through the activation of Nrf2 in NRCMs. A: Fold changes in *Nrf2*, *Ugt1a1* and *1a9* mRNA levels by real-time RT-PCR in Nrf2 siRNA transfected NRCMs combined with indicated treatments. B: Representative Western blots of NRF2, UGT1A1 and UGT1A9 in whole lysates and fold changes in relative densitometric values in NRCMs subjected to the indicated treatments. * $P < 0.05$ *vs*. Control + negative control (NC) siRNA group; $^{\#}$ $P < 0.05$ *vs*. AngII + negative control (NC) siRNA group, § $P < 0.05$ vs. AngII +Puerarin + negative control (NC) siRNA group, $^{\vartriangle}$ $P < 0.05$ *vs*. Puerarin + negative control (NC) siRNA group, n=6 for each group.

JPET Fast Forward. Published on June 26, 2018 as DOI: 10.1124/jpet.118.248369
This article has not been copyedited and formatted. The final version may differ from this version.

Fig. 8 Puerarin enhanced Nrf2 binding to UGT1A1 and UGT1A9 promoter regions. A: Nucleotides marked red show a high information content, which in capital letters denotes the core sequence used by Matlnspector software. Genomic binding sites were identified by ChIP-Seq. B and C: Sequences of *Ugt1a1* and *Ugt1a9* promoters. D and E: Chromatin was immunoprecipitated with anti-NRF2 antibody, positive control anti-RNA Polymerase II and negative control normal mouse IgG. Nrf2 binding to *Ugt1a1* or *1a9* promoter was determined by qPCR with *Ugt1a1* or *1a9* specific primers. The same primers were also used to amplify *Ugt1a1* or *1a9* promoter regions to show 1% input DNA. Graphic representation of the results obtained in ChIP-qPCR with the "percent input" method. *: $P<0.05$ vs. NC group, #: $P<0.05$ vs. Cont+anti-NRF2 group, n=6 for each group.

Table

	Sham	AAC	AAC+Pue	Pue
SBP (mmHg)	122.8±5.8	149.5±13.9 *	132.9±11.1 #	124.1±3.9 #
DBP(mmHg)	95.6±7.9	120.1±12.9 *	98.7±10.5 #	96.4±5.3 #
LVESP (mmHg)	114.8±13.5	144.2±10.4 *	121.2±14.8 #	116.6±18.9 #
LVEDP (mmHg)	5.1±2.6	5.5±3.2	5.3±2.9	5.3±2.9
Max +dp/dt (mmHg/s)	4078±587	4289±1141	3835±884	3881±497
Max -dp/dt (mmHg/s)	-3667±629	-3471±1492	-3576±1109	-3481±389

Table 1 Hemodynamic parameters in rats without or with puerarin administered 6 weeks post-surgery. LVESP, left ventricular end-systolic pressure; LVEDP, left ventricular end-diastolic pressure; Max +dp/dt , maximal rate of pressure development; Max -dp/dt, maximal rate of pressure decay. Systolic blood pressure(SBP) and diastolic blood pressure(DBP) detected by rat tail artery blood pressure mesurement. *$P < 0.05$ *vs*. sham group; #$P < 0.05$ *vs*. AAC group, n=8.

JPET Fast Forward. Published on June 26, 2018 as DOI: 10.1124/jpet.118.248369
This article has not been copyedited and formatted. The final version may differ from this version.

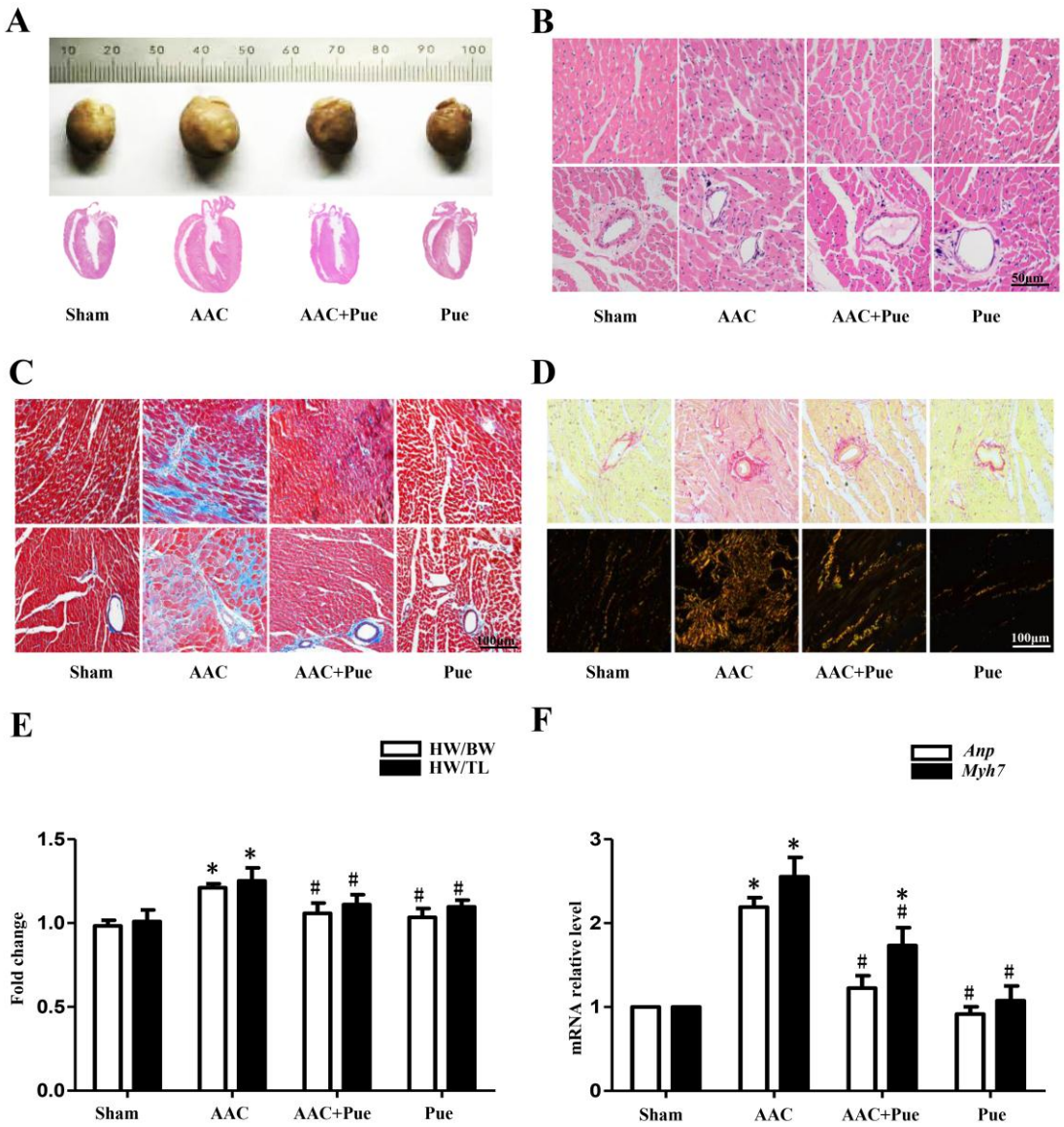

Figure 1.

JPET Fast Forward. Published on June 26, 2018 as DOI: 10.1124/jpet.118.248369
This article has not been copyedited and formatted. The final version may differ from this version.

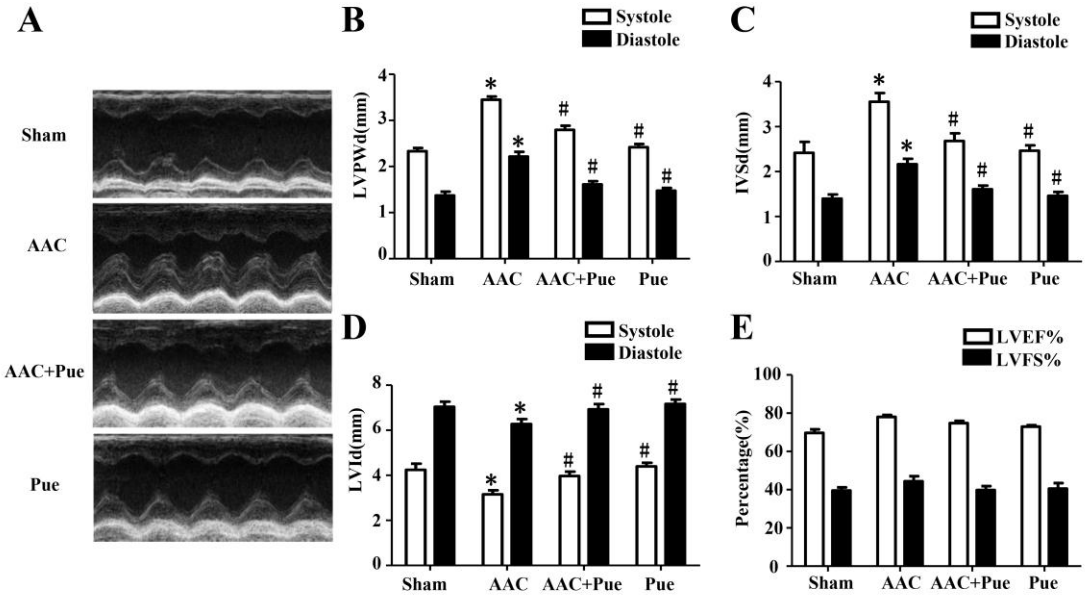

Figure 2.

JPET Fast Forward. Published on June 26, 2018 as DOI: 10.1124/jpet.118.248369
This article has not been copyedited and formatted. The final version may differ from this version.

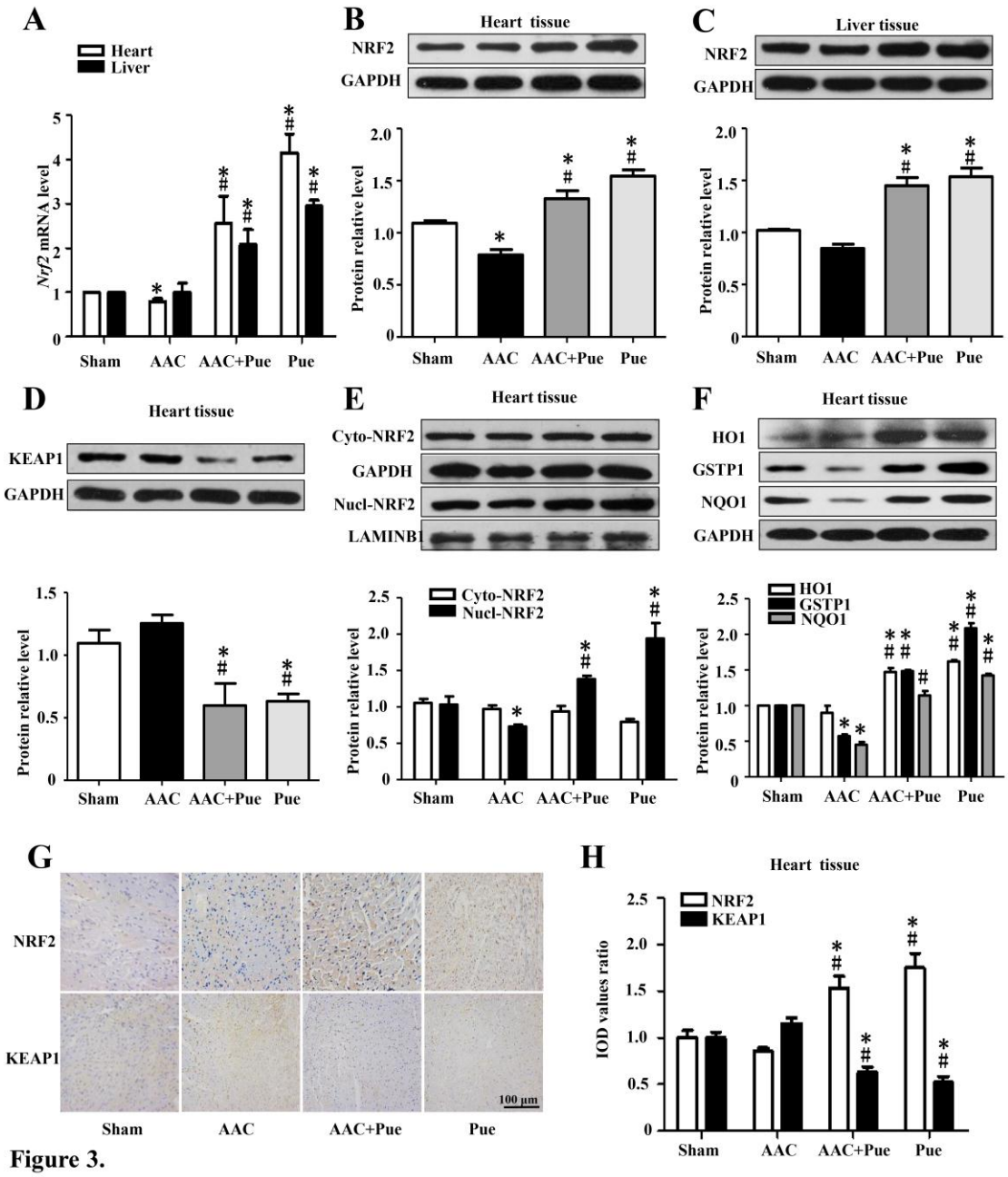

Figure 3.

JPET Fast Forward. Published on June 26, 2018 as DOI: 10.1124/jpet.118.248369
This article has not been copyedited and formatted. The final version may differ from this version.

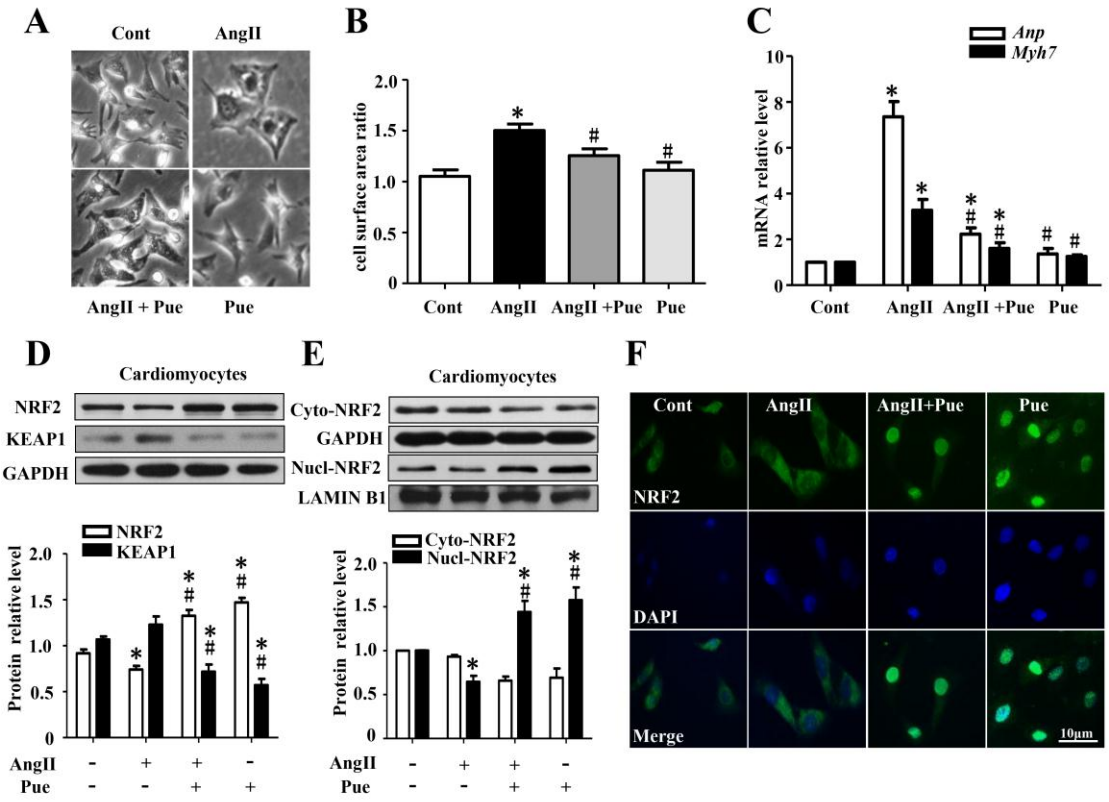

Figure 4.

JPET Fast Forward. Published on June 26, 2018 as DOI: 10.1124/jpet.118.248369
This article has not been copyedited and formatted. The final version may differ from this version.

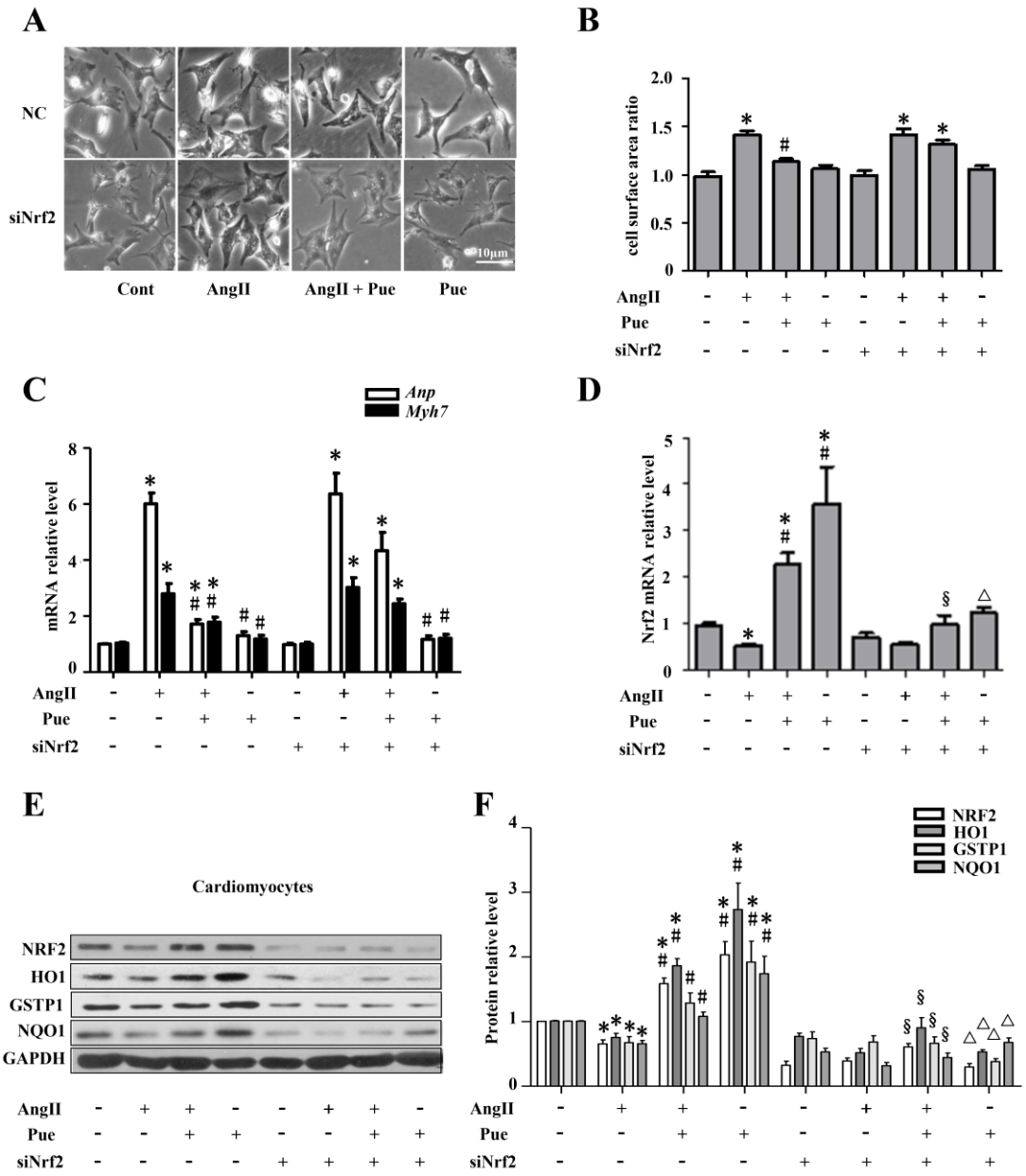

Figure 5.

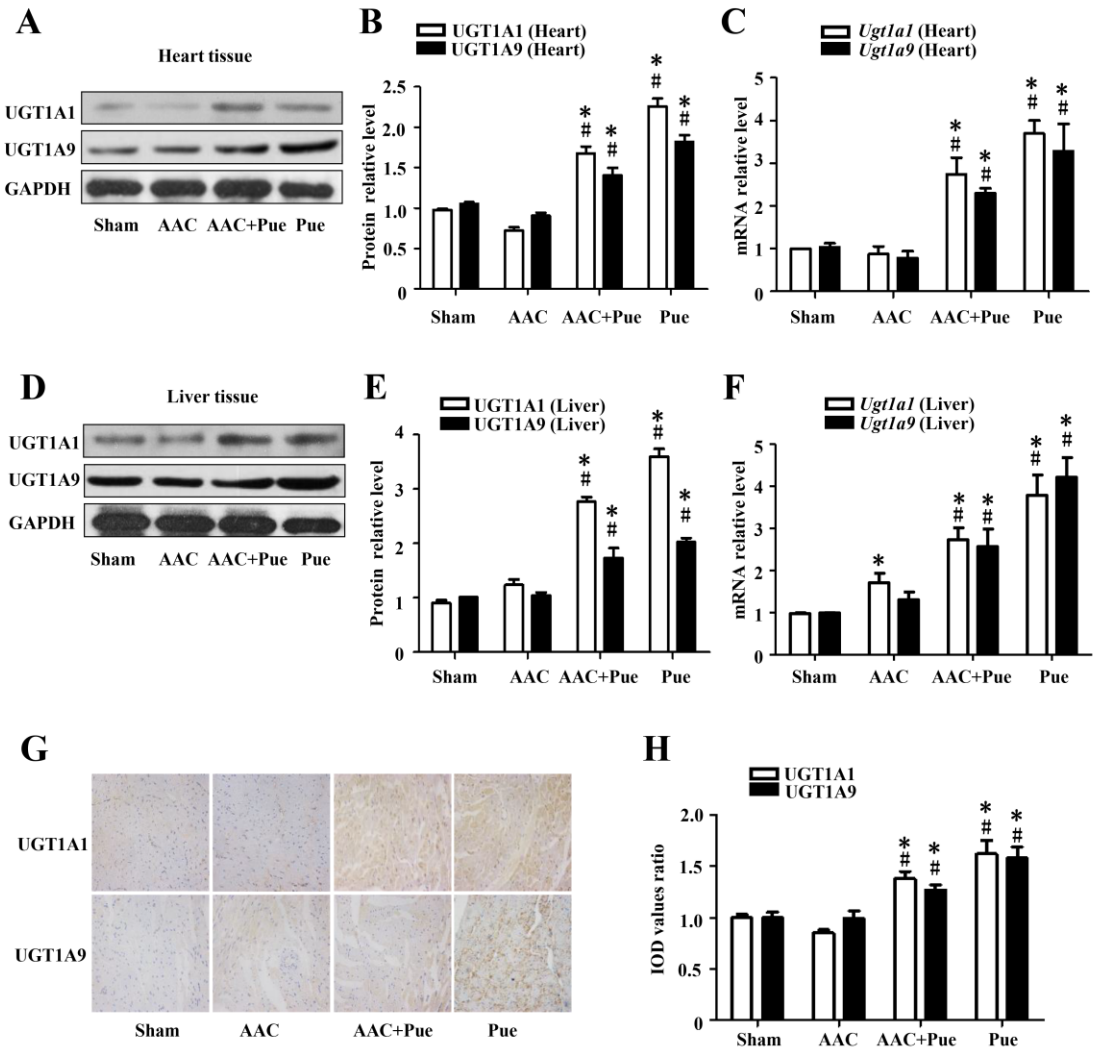

Figure 6.

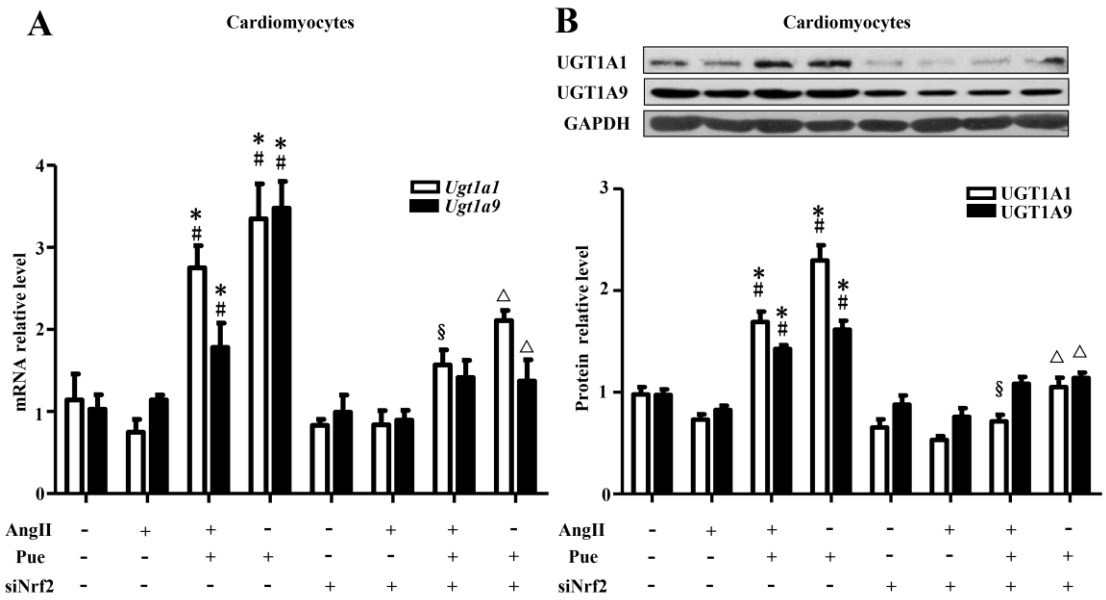

Figure 7.

JPET Fast Forward. Published on June 26, 2018 as DOI: 10.1124/jpet.118.248369
This article has not been copyedited and formatted. The final version may differ from this version.

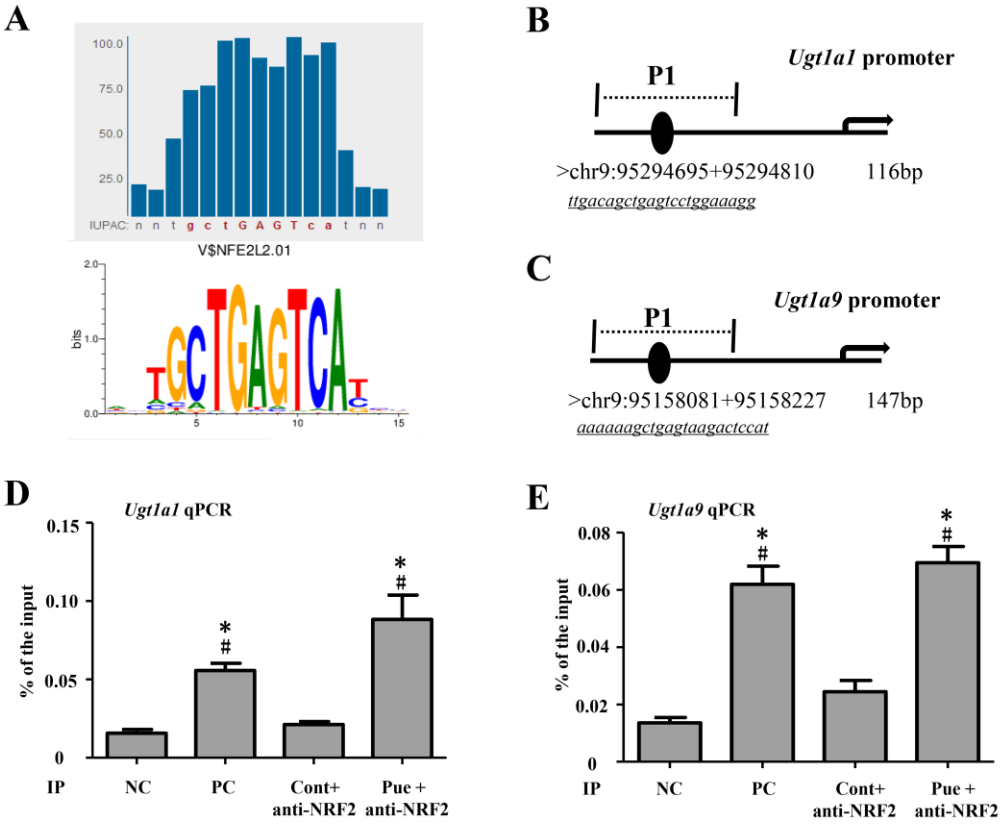

Figure 8.